Progress of indirect drive inertial confinement fusion in the United States

OPEN ACCESS
IOP Publishing | International Atomic Energy Agency
Nuclear Fusion
Nucl. Fusion **59** (2019) 112018 (11pp)
https://doi.org/10.1088/1741-4326/ab1ecf

Progress of indirect drive inertial confinement fusion in the United States

J.L. Kline[1], S.H. Batha[1], L.R. Benedetti[2], D. Bennett[2], S. Bhandarkar[2], L.F. Berzak Hopkins[2], J. Biener[2], M.M. Biener[2], R. Bionta[2], E. Bond[2], D. Bradley[2], T. Braun[2], D.A. Callahan[2], J. Caggiano[2], C. Cerjan[2], B. Cagadas[2], D. Clark[2], C. Castro[2], E.L. Dewald[2], T. Döppner[2], L. Divol[2], R. Dylla-Spears[2], M. Eckart[2], D. Edgell[4], M. Farrell[3], J. Field[2], D.N. Fittinghoff[2], M. Gatu Johnson[5], G. Grim[2], S. Haan[2], B.M. Haines[1], A.V. Hamza[2], EP. Hartouni[2], R. Hatarik[2], K. Henderson[2], H.W. Herrmann[1], D. Hinkel[2], D. Ho[2], M. Hohenberger[2], D. Hoover[3], H. Huang[3], M.L. Hoppe[3], O.A. Hurricane[2], N. Izumi[2], S. Johnson[2], O.S. Jones[2], S. Khan[2], B.J. Kozioziemski[2], C. Kong[2], J. Kroll[2], G.A. Kyrala[1], S. LePape[2], T. Ma[2], A.J. Mackinnon[2], A.G. MacPhee[2], S. MacLaren[2], L. Masse[2], J. McNaney[2], N.B. Meezan[2], J.F. Merrill[1], J.L. Milovich[2], J. Moody[2], A. Nikroo[2], A. Pak[2], P. Patel[2], L. Peterson[2], E. Piceno[2], L. Pickworth[2], J.E. Ralph[2], N. Rice[3], H.F. Robey[2], J.S. Ross[2], J.R. Rygg[4], M.R. Sacks[1], J. Salmonson[2], D. Sayre[2], J.D. Sater[2], M. Schneider[2], M. Schoff[3], S. Sepke[2], R. Seugling[2], V. Smalyuk[2], B. Spears[2], M. Stadermann[2], W. Stoeffl[2], D.J. Strozzi[2], R. Tipton[2], C. Thomas[2], RPJ Town[2], P.L. Volegov[1], C.Walters[2], M. Wang[2], C. Wilde[1], E. Woerner[2], C. Yeamans[2], S.A. Yi[1], B. Yoxall[2], A.B. Zylstra[2], J. Kilkenny[3], O.L. Landen[2], W. Hsing[2] and M.J. Edwards[2]

[1] Los Alamos National Laboratory, Los Alamos, NM, United States of America
[2] Lawrence Livermore National Laboratory, Livermore, CA, United States of America
[3] General Atomics, San Diego, CA, United States of America
[4] Laboratory for Laser Energetics, Rochester, NY, United States of America
[5] Massachusetts Institute of Technology, Boston, MA, United States of America

E-mail: jkline@lanl.gov

Received 24 December 2018, revised 29 March 2019
Accepted for publication 2 May 2019
Published 24 July 2019

Abstract

Indirect drive converts high power laser light into x-rays using small high-*Z* cavities called hohlraums. X-rays generated at the hohlraum walls drive a capsule filled with deuterium–tritium (DT) fuel to fusion conditions. Recent experiments have produced fusion yields exceeding 50 kJ where alpha heating provides ~3× increase in yield over PdV work. Closing the gaps toward ignition is challenging, requiring optimization of the target/implosions and the laser to extract maximum energy. The US program has a three-pronged approach to maximize target performance, each closing some portion of the gap. The first item is optimizing the hohlraum to couple more energy to the capsule while maintaining symmetry control. Novel hohlraum designs are being pursued that enable a larger capsule to be driven symmetrically to both reduce 3D effects and increase energy coupled to the capsule. The second issue being addressed is capsule stability. Seeding of instabilities by the hardware used to mount the

capsule and fill it with DT fuel remains a concern. Work reducing the impact of the DT fill tubes and novel capsule mounts is being pursed to reduce the effect of mix on the capsule implosions. There is also growing evidence native capsule seeds such as a micro-structure may be playing a role on limiting capsule performance and dedicated experiments are being developed to better understand the phenomenon. The last area of emphasis is the laser. As technology progresses and understanding of laser damage/mitigation advances, increasing the laser energy seems possible. This would increase the amount of energy available to couple to the capsule, and allow larger capsules, potentially increasing the hot spot pressure and confinement time. The combination of each of these focus areas has the potential to produce conditions to initiate thermo-nuclear ignition.

Keywords: inertial fusion, indirect drive, laser fusion, inertial fusion energy

(Some figures may appear in colour only in the online journal)

1. Introduction

Indirect drive (ID) inertial confinement fusion (ICF) converts high power laser light into x-rays traditionally using small cylindrically-shaped, high-*Z* radiation cavities called hohlraums. A spherical capsule placed at the center of the hohlraum containing deuterium–tritium (DT) fuel absorbs x-rays ablating the outer surface of the capsule and imploding via rocket motions. For 'hot spot' ignition, the primary approach to high gain ICF [1], the capsule has a layer of DT ice just inside the capsule with residual DT gas filling the central cavity. The capsules have traditionally been made of plastic (CH) or beryllium [2–6], but recently high density carbon (HDC) became the standard capsule material for experiments on the National Ignition Facility (NIF). Compression of the DT gas forms a central 'hot spot' where the fusion is initiated and under the right conditions is self-heating by capturing the alpha particles from the fusion reactions far exceeds the cooling mechanisms, causing the hot spot to ignite. Once a robust burning plasma is formed in the 'hot spot', ablation and heating of the inner surface of ice layer begins a propagating burn generating multi-megajoule neutron yields.

Since the completion of the NIF [7] and cryogenic target capabilities came online in 2010 [8, 9], much progress has been made towards ignition with more than a 20× increase in fusion neutron production and a three times increase in 'hot spot' pressure, as well as significant enhancements in diagnostic capabilities to understand capsule and hohlraum performance, and advancement in laser facility optics damage mitigation techniques and precision. Early experiments using high-gain (defined as the ratio of the output neutron energy to the laser input energy) target-designs [10] highly optimized for peak performance, fell well below expectation. These experiments under-performed due to the combination of 3D effects such as high mode 4-pi mix [11–15] and low mode asymmetries [16] amplified by high convergence [17, 18]. Experiments following the initial high gain target designs traded gain for improved performance. The experiments included the 'high foot' campaign [19], which increased the power in the initial portion of the laser pulse called the 'foot', shown in figure 1 with a low foot pulse in black and a high foot pulse in red. The increased power in the 'foot' of the pulse has three primary effects: smoothing initial seeds for ablative hydrodynamic instability, increasing the scale-length of the ablation-front, and increasing the internal energy of the fuel reducing the theoretical compression and convergence. These experiments improved the performance by more than an order of magnitude and demonstrated self-heating of the 'hot spot' for the first time in ICF [20–22]. However, the 'high foot' implosions were ultimately limited in performance by laser backscatter reducing the amount of drive available for the targets and time-dependent cross-beam energy transfer affecting symmetry control [23–27], as well as feature driven shell perforations due to the tent [28–30]. Summaries of this work can be found in references by Meezan *et al* [31] and Edwards *et al* [17].

Over the past few years, target design changes have advanced implosion performance. Moving to low gas filled hohlraums significantly reduced backscatter, increasing the drive available to the target as well as reducing laser damage concerns; has reduced by two orders of magnitude the production of suprathermal electrons inside the hohlraum, and improved time-dependent symmetry control by reducing cross-beam transfer allowing implosion symmetry to be controlled directly through changes in the laser beam power balance. As opposed to the silicon-doped plastic-capsules used for the low and high 'foot' campaigns, the introduction of HDC capsules [33–36] enables higher velocity implosions with higher fuel internal energy that can still theoretically produce high gain. Many of these improvements can be attributed to the shorter laser pulse required for HDC capsules (figure 1). Top-performing implosions now regularly exceed 50 kJ of fusion output in a regime where the yield is dominated by self-heating via the alpha particles produced from the fusion reactions and 'hot spot' pressures of ~300 Gbar, near ignition relevant conditions [37–39]. While the yield performance of ID implosions on NIF have improved by more 20×, there are still significant challenges to reaching ignition.

Moving forward, there will be a two pronged approach to increase performance of the current implosions. Improvements in the implosions quality by reducing remaining 3D effects such as low mode asymmetries and mix have the potential to

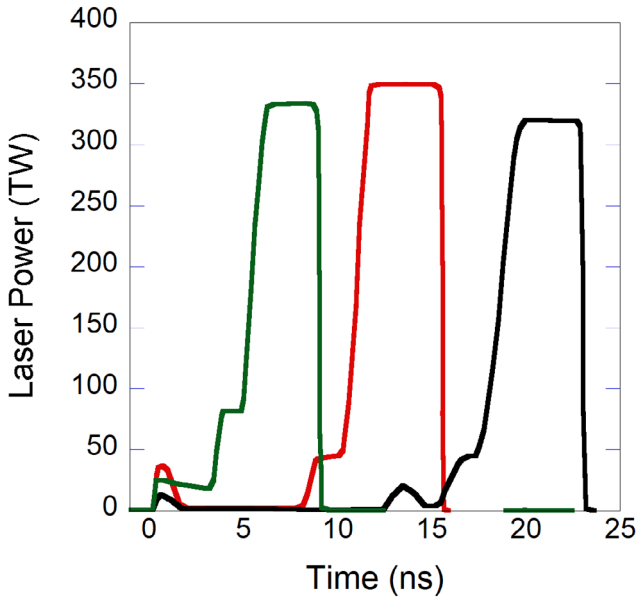

Figure 1. Example laser pulse shapes for a low foot (N120321), a high foot (N130612), and a three-step HDC pulse (N141019) shape [32].

increase performance rapidly for small improvements. The second approach is to increase the size of the capsule increasing its absorbed energy while still controlling the implosion symmetry and maintaining implosion velocity. Scaling to larger capsule sizes also improves the no alpha burn performance as $S^{4.5}$, where S represents the scale factor and no alpha burn means the increased performance does not include alpha heating. Once alpha heating is included, the yield performance exceeds the $S^{4.5}$ scaling. Unless the symmetry for larger capsules can be controlled using the current hohlraum size, increasing the capsule size will require an increase in hohlraum size which means additional laser energy will be needed which scales as $\sim E_{\mathrm{L}} * S^3$, where E_{L} is the laser energy for the original unscaled target. This paper lays out the current understanding of the performance of indirect drive ICF implosions on the NIF and the approach to both improving performance as well as understanding what steps are needed to achieve ignition. The paper will be broken into a description of the current target designs in section 2, issues and plans to improve implosions qualtiy in section 3, and both high and low mode asymmetries and scaling the current designs up in section 4.

2. Current status

Over the past few years, the principle effort is focused on low gas filled hohlraums with HDC capsules (figure 2). The best performing designs hinge around a 70 μm thick HDC capsule with an inner radius of 910 μm and ice layer thickness of ~56 μm. The capsules use a 20 μm thick doped layer with a few tenths of a percent of tungsten dopant. The dopant layer shields the DT ice layer from hard x-rays generated by the laser interactions with the hohlraum wall and is designed to reduce decompression of the inner capsule region to improve the hydrodynamic stability of the fuel-capsule interface. Work in ongoing to optimize the dopant layer in terms of thickness and dopant percentage. The capsule is placed at the center of a gold hohlraum with a 6.20 mm diameter and a length of 11.3 mm. The laser entrance holes have a 3.70 mm diameter. With ~1.7 MJ of laser energy and a peak power of ~450 TW, implosions have achieved greater than 50 kJ of neutron energy with hot spot pressures of ~300 Gbar.

For the best performing implosions, the conditions in the central hot spot can be deduced from the measurements and compared to the generalized Lawson criteria [40] for ICF [41, 42]. Using one of the best implosions [37] with an ion temperature of 4.5 ± 0.15 keV and a down scattered ratio (DSR)[6] of 0.0324 ± 0.002 that translates to a total areal density of $21 * \mathrm{DSR} = 0.68 \pm 0.04$ g cm^{-2}, the performance is ~70% of that needed to reach ignition.

Advantages of HDC capsules compared to other ablators such as the use of shorter laser pulses, advantageous for symmetry control in low gas filled hohlraums, the ability to reach high implosion velocities, and a smooth surface finishes to reduce ablative hydrodynamic instabilities seeds have made it the principle target design ablator. HDC capsules performance exceed all past target designs using plastic or beryllium making it the principle focus at present in the march towards ignition. While gains have been made using HDC, there is still more work to do to either improve the quality of the capsule implosions or scale the capsule up in size.

Beryllium and plastic (CH) ablators remain potential candidates for future target designs. The ablation rate of beryllium enable designs at lower radiation temperatures taking advantage of ablative stabilization. This property could enable exploration of a larger capsules in a bigger hohlraum where the radiation drive is reduced due to laser energy and power limits. Experiments have shown good symmetry control in low gas filled hohlraums [43, 44] and good performance for subscale DT layered implosions [45]. However, challenges remain for the beryllium capsule quality. The current strategies for reducing the 3D effects and improved hohlraum designs applies directly to both beryllium as well as plastic. The lower density of these ablators require longer laser pulses which may require improved hohlraums.

The efforts focused on improving the performance of HDC capsules applies to other ablator materials with which the program has less experience. Regardless of the ablator material controlling 3D effects is critical to reducing the energy necessary to reach ignition. Likewise, determining how to drive larger capsules moves towards ignition. Once these approaches have been maximized, the trade-offs between ablator materials may be valuable.

3. Quality

The path forward to reduce the required laser energy to achieve ignition is to generate '1D like' implosions. Such implosions can be driven to higher velocities and convergences leading to higher performance. Therefore, one of the key research focuses is reducing the sources of 3D imperfections [28]. The

[6] DSR is a measure of the fuel areal density and defined as the ratio of the measured neutrons with energies of 10–12 MeV to those with 13–15 MeV.

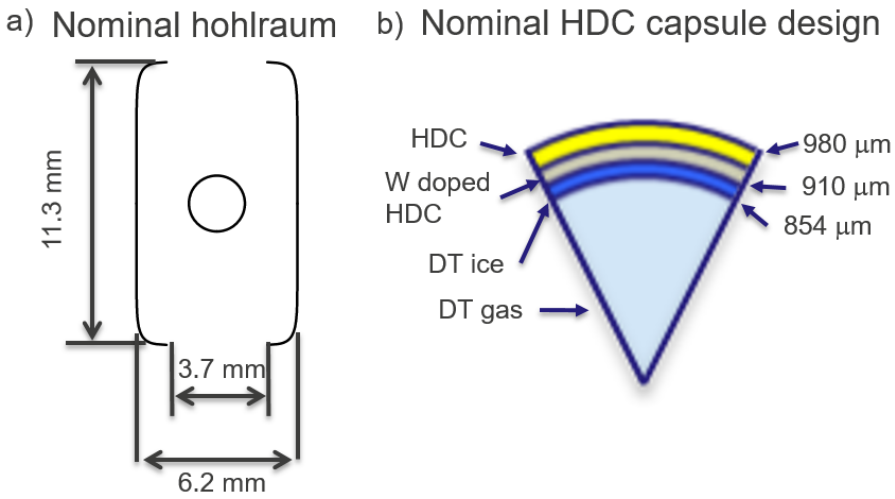

Figure 2. Nominal (*a*) hohlraum and (*b*) capsule schematic for HDC targets.

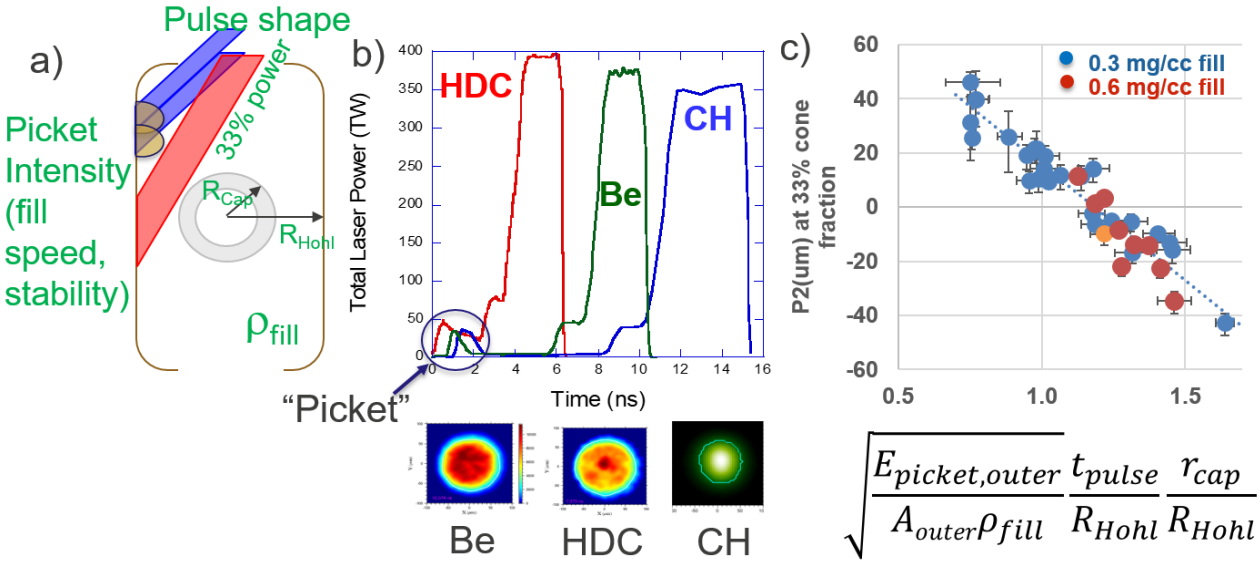

Figure 3. (*a*) Schematic of the hohlraum showing inner and outer cone beams with respect to the plasma expansion of the gold wall and capsule. (*b*) Pulse shapes and x-ray self-emission for a HDC (N160221 [50], a beryllium (N170314 [44], and a CH capsule. Reprinted from [50], with the permission of AIP Publishing. (*c*) Plot of corrected symmetry versus empirical metric.

3D effects are split into low mode asymmetries and high mode effects which can be further categorized as feature driven perturbations, perforations, or mix due to capsule mounting hardware and fill tube or intrinsic 4-pi hydrodynamic instabilities such as Rayleigh–Taylor or Richtmyer–Meshkov that occur at interfaces.

3.1. Low mode

As the ID campaign moved to low gas filled hohlraums, control of implosion symmetry vastly improved with improved consistency between the simulations and measurements, i.e. substantially reduced multipliers on the input laser power as with the gas filled hohlraum, as well as an empirical understanding making the designs more predictable. For ID targets, control of implosion symmetry depends on the ability to deposit the laser energy in the hohlraum at the desired locations. The NIF laser is split into outer cone beams incident at 44.5 and 50 with respect to the hohlraum axis and the inner cone beams at 23.5 and 30 with respect to the hohlraum axis. The outer cone beams are pointed at the hohlraum wall just inside the laser entrance holes while the inner cone beams are pointed to the waist of the hohlraum as in figure 3. Symmetry control requires an understanding of the hohlraum dynamics that dictate the radiation pattern on the capsule. The dynamic nature of the hohlraum as the intense lasers ablate material of the hohlraum wall leads to time dependent changes that affect where the laser beams deposit their energy [46]. The principal challenge is propagation of the inner cone laser beams to the waist of the hohlraum. As shown in figure 3(*a*), expansion of the gold plasma ablated from the hohlraum by the laser pointed just inside the laser entrance holes, known as the 'gold bubble', begins to block the path of the inner cone beams [47, 48]. Material ablated from the surface of the capsule also blows-off into the path of the inner cone beams. The work of Callahan *et al* [49]

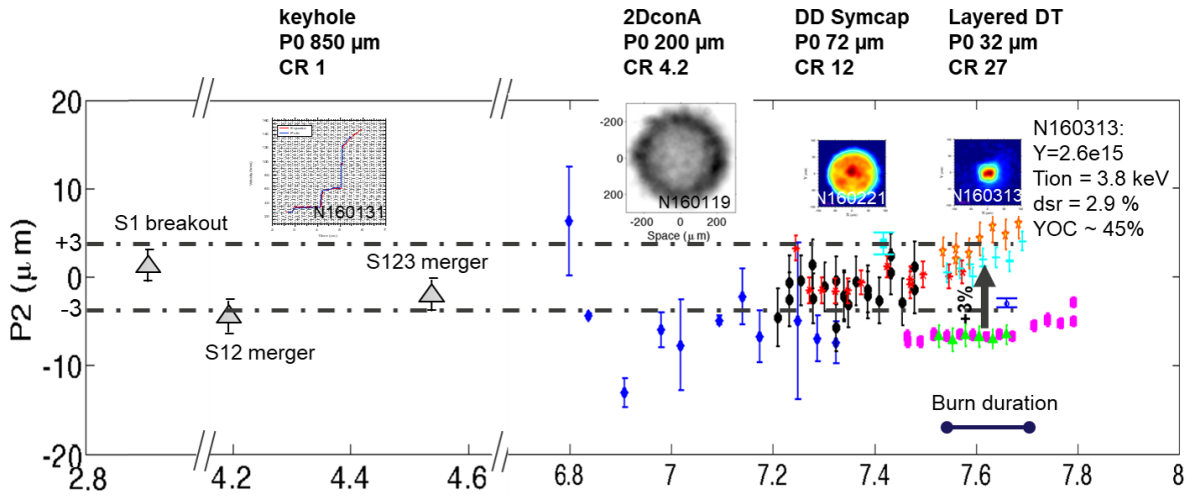

Figure 4. Data from VISAR early in time, backlight radiography of the capsule during the implosion, x-ray self-emission from symcaps and layered DT implosions show the symmetry with the low gas-filled hohlraums remains nearly round.

shows an empirical relationship for implosion shape in a hohlraum derived from experimental values:

$$\sqrt{\frac{E_{\text{picket,outer}}}{A_{\text{outer}}\rho_{\text{fill}}}}\frac{t_{\text{pulse}}}{R_{\text{Hohl}}}\frac{r_{\text{cap}}}{R_{\text{Hohl}}}$$

where $E_{\text{picket,outer}}$ is the laser energy in the picket and main outer cone portion of the pulse, A_{outer} is the wall illumination area by outer cone beams, ρ_{fill} is the gas fill density, τ_{pulse} is the total length of the laser pulse, R_{Hohl} is the radius of the hohlraum, r_{cap} is the radius of the capsule. The terms $r_{\text{cap}}/R_{\text{Hohl}}$ and $\tau_{\text{pulse}}/R_{\text{Hohl}}$ address expansion of the capsule and wall respectively. The formula represents physical processes that affect the symmetry in the hohlraum. The energy in the initial part of the laser known as the 'picket' (figure 3(*b*)) drives early time gold plasma blow-off and setups up initial plasma conditions for the energy in the main pulse. The energy in the main pulse and the area covered by the laser determine the dynamics of the gold bubble expansion that impede the inner cone laser beams from reaching the waist of the hohlraum. $\tau_{\text{pulse}}/R_{\text{Hohl}}$ describes the relationship between pulse length which determines the expansion time for the gold bubble and the distance the bubble has to expand before impeding inner code beams. Shorter laser pulses or larger hohlraum radii at the outer cone beams help inner cone beam propagation. $r_{\text{cap}}/R_{\text{Hohl}}$ captures how much space between the wall and the capsule because the capsule blow-off that also affects inner cone beam propagation. Expansion of both the wall and the capsule plasma block the inner cone beams from reaching the locations they are pointed. The final factor that determines the gold bubble expansion dynamics is the use a low density gas fill $<0.6\,\text{mg cc}^{-1}$ which provides plasma pressure increasing resistance for the gold bubble expansion. The fill density is limit to $<0.6\,\text{mg cc}^{-1}$ to ensure both laser plasma instabilities and well as cross beam energy transfer remains negligible [51], since both have a direct dependence on plasma density. The empirical relationship derived based on data is not dimensionless and exponents used are based on fits the data.

Application of this formula to the data produces a linear relationship with the capsule shape as shown in figure 3(*c*) as published in [49]. Development of the relationship between shape and the empirical formula uses sets of data at the same gas fill density and transforms the measured P2 Legendre polynomial coefficient to the coefficient that corresponds to the expected shape for a 33% cone fraction, defined as ratio of inner cone power to total power. The transformation is linear with cone fraction based on the different between the experimental and a 33% cone fraction. This process essentially normalizes the cone fraction for all experiment for a 1-to-1 comparison and would not be possible using the same liner adjustment to the shape with cone fraction if the hohlraums did not behave in a predictable manner [52]. In addition to experimental data, the empirical shape scaling is consistent with simulations. The rationale for adjusting to a 33% cone fraction for comparisons is that a 33% cone fraction permits optimal use of NIF's power and energy due to the ratio of inner to outer cone beams. It should be noted that data also suggests the trend is relatively independent of the capsule material.

Controlling the capsule implosion symmetry is more than producing a nearly round implosion at peak compression. Preventing swings in the symmetry throughout the pulse is also important since energy in the swings reduces drive efficiency [53]. The low gas-filled hohlraum provides direct control of time-dependent implosion symmetry through adjusting the requested laser beam power balance rather than depending on time-dependent cross-beam energy transfer determined by evolving laser entrance hole plasma conditions. Data measured with principal diagnostics at different times through the laser pulse indicate the symmetry can be controlled with only minor swings in shape as shown in figure 4 [50].

While the shape of the x-ray self-emission and neutron pinhole measurements show the final hot spot shape can be controlled at the level believed to be needed for ignition, measurements suggest asymmetry in the compression of the cold fuel and potentially bulk motion of the capsule

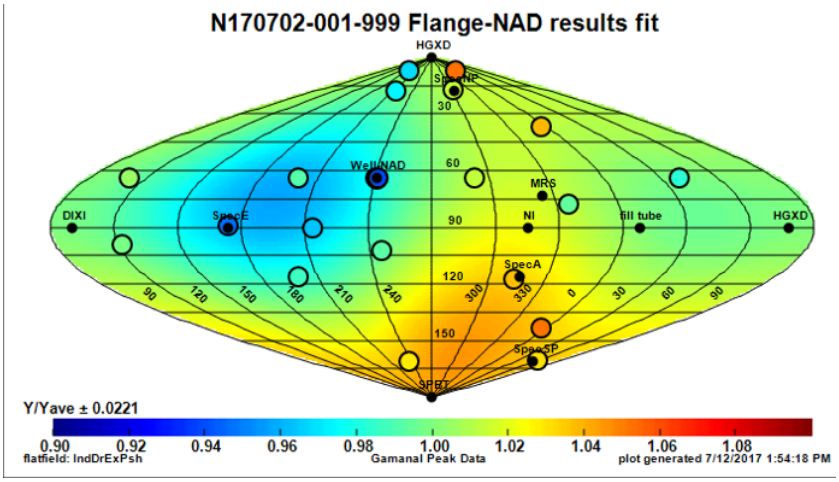

Figure 5. Map of the neutron yield variations as measured by the neutron flux measured by the NADs placed at different locations around the target chamber denoted by the circles for shot N171029.

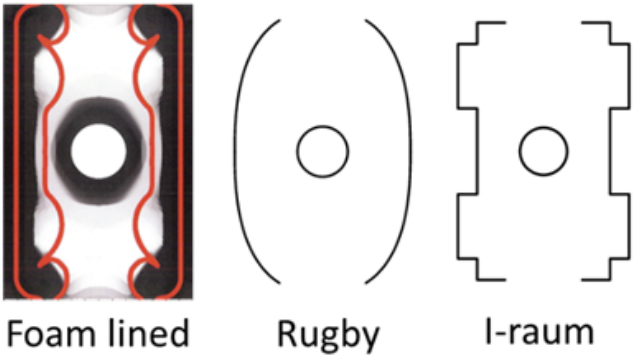

Figure 6. Three hohlraum designs being pursued to enable symmetry control for longer laser pulses.

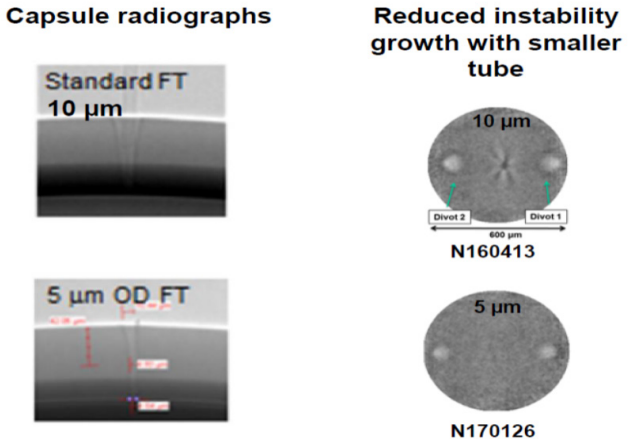

Figure 7. Experimental data from experiments comparing 10 and 5 μm file tubes showing (*a*) capsule radiographs prior to shots, (*b*) hydrogrowth radiography data for shots N160413 (10 μm) and N170126 (5 μm) [79].

[54]. These asymmetries may be comprised of a combination of both asymmetries arising from late time control due to beam propagation in the hohlraum or 3D effects due to the laser-target system which would require different solutions to improve the quality of the implosions. Figure 5 shows an example of the measurements using neutron activations diagnostics (NADs) [55, 56] at various locations around the NIF target chamber. NADs measure the absolute number of neutrons above a given threshold through interacting of the neutrons with a high-Z activation foil. The neutron flux through each foil can be determined by counting the decay of the radioactive nuclei from the foil. Based on the measured flux from the NADS, the number of 14 MeV neutrons produced by an implosion can be measured in the direction of each foil. Reconstruction of the flux measured by each foil and its position around the chamber is used as a measure of the areal cold fuel density since the flux is reduced by neutron collision in the dense fuel depending on the ρR, where ρ is density and R is the thickness of the fuel in a given direction. The reconstruction shown in figure 5 for shot 170702-001 shows a common variation in the fuel thickness with higher flux, or thinner ice, is represented by red and lower flux, or thicker ice is represented by blue. The neutron flux variations are attributed to variations in the ρR (density $\times$ thickness) in the ice layer. Further analysis of the signals measured by the neutron time of flight detectors [57, 58] show that there is also bulk motion of the capsule [59, 60]. Before these asymmetries can be mitigated, their respective sources must be understood and diagnosed, which remains an important component of current programmatic efforts. Efforts to reconstruct the ice layer density using three orthogonal neutron images are being developed. The neutron imaging systems [61] can measure both the neutrons generated by fusion reactions in the hot spot called the primary neutrons, as well as the neutron scattered by the cold compressed fuel called the downscattered neutrons. Since the downscattered neutrons lose energy, an image gating system is used to discern the two populations of neutrons. Using both the primary and downscattered neutron images from three lines of site the shape of the cold fuel can be reconstructed [62]. In addition, imaging of the compressed cold fuel by short pulse point projection radiography based on Compton scattering of high energy x-rays is under development [63, 64].

In addition to improved diagnostics, engineering and scientific teams have been examining other potential sources of

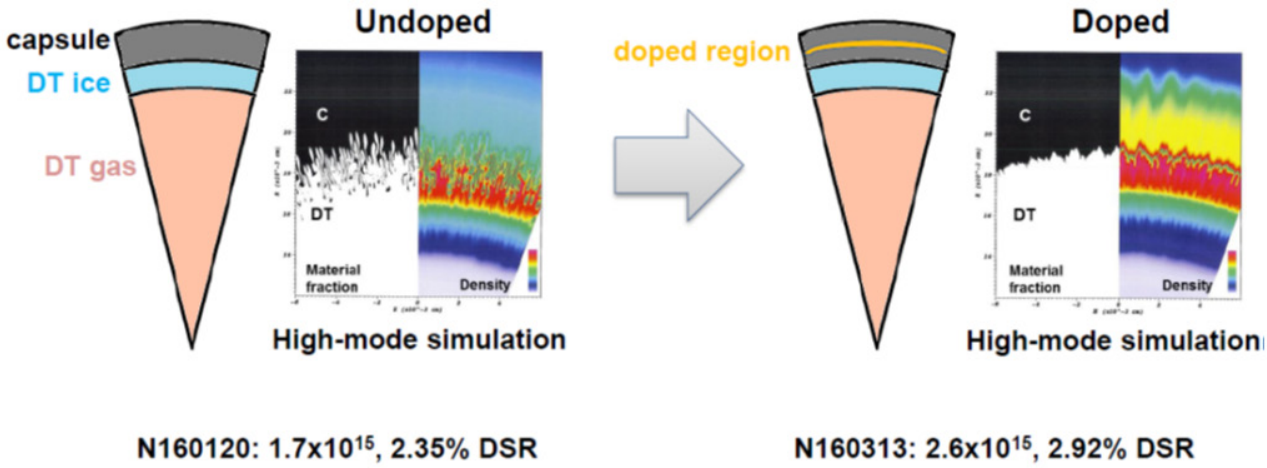

Figure 8. Data and simulations for a comparison of variation in tungsten dopant for HDC DT layered experiments showing improve performance with dopant and simulations that show the dopant stabilizes interface [87].

asymmetries. For instance, just prior to the laser being fired, a set of shrouds used to block IR radiation from the chamber needed to control the target temperature near the DT triple point open. Vibrations due to the shroud opening are expected to damp-out prior to the shot. However, there are some indications this may not be true causing the target to move from its originally aligned position. Other potential issues are also being examined such as small laser peak power imbalances, power balance during the foot of the laser pulse, and diagnostic holes in the target [65, 66]. While these effects may produce small improvements of the current symmetry, they may account for an estimated ~1.5× improvement in performance at the current levels of alpha heating [54, 67].

The basic understanding in low gas filled hohlraums has led to improved performance. To capitalize on the knowledge to make the next advance in performance, modifications to the hohlraum design are in progress to improve late-time symmetry control, one of the limiting factors believed to further improvement in symmetry control for longer laser pulse lengths. Figure 6 shows the leading candidates including foam liners [68, 69], rugby hohlraums [70–73], and the I-raum [74]. The foam lined hohlraums use pressure from the heated foam material to slow the wall expansion. The alternate hohlraum shape/geometry concepts enable the inner beam lasers to propagate to the designed location for longer laser pulses needed to implode larger capsules while controlling symmetry. The rugby hohlraum offer the potential for the most gain by not only controlling symmetry but coupling significantly more energy to the capsule. However, more work is needed to demonstrate these improvements and ensure laser plasma instabilities do not erase all gains.

3.2. High mode asymmetries

Mixing at the ablator/ice interface or ice/gas interface are the toughest challenges in mitigating the 3D nature of the implosions. It has long been know that mixing of the ablator and ice into the hot spot occurs as a result of surface roughness and engineering features such as the fill tube and tent used to mount the capsule in the hohlraum [29, 30]. The strategy to mitigate the effect of the 3D engineering features for indirectly driving implosions is to reduce the perturbation seed [75, 76]. For instance, the original fill tubes were 10 μm in diameter. Recently, the size has been reduced to 5 μm which has had a notable effect on performance. As shown in figure 7, measurements using the hydro-growth radiography platform (HGR) [77] to measure the growth of perturbation show a notable reduction in growth due to the fill tube [68, 69, 78, 79]. This is consistent with x-ray self-emission observations as well. Using the 5 μm fill tube on DT layered implosions has shown notable improvement in performance outside uncertainty bands [80], and development of a 2 μm fill tube is in progress. Similarly, there are several concepts to mitigate the capsule mounting hardware [81]. Tents designed to cover a smaller region near the capsule poles [82], small wire supports, or low density materials to separate mounting hardware from capsule.

Other target characteristics such as surface roughness, internal ablator structure, and dopants are sources of hydrodynamic instabilities that degrade performance through mixing the shell or DT ice into the hot spot quenching the burn. The introduction of HDC [83, 84] ablators have reduced ablative hydrodynamic instabilities as a result of the high radiation temperature x-ray drives and improve surface finish which reduces the initial instability seeds [85]. This enables higher velocity implosions that have a strong dependence on performance by enabling a larger ratio of the initial to final fuel mass, $v \sim \ln(m_f/m_i)$ where v is velocity m_f is the final ablator mass and m_i is the initial ablator mass. That being said, the high convergences of the capsule implosions do make the performance sensitive to seeds for mix since the effects are amplified by compression [86]. Moreover, direct measurement of the instability growth in spherical geometry at high convergence is very challenging. Understanding 4π mix driven by hydrodynamic instabilities that occur at each interface and cover 4π steradians of the interface is challenging. 4π mix is typically understood through simulations and inferred through performance measured in experiments. For instance,

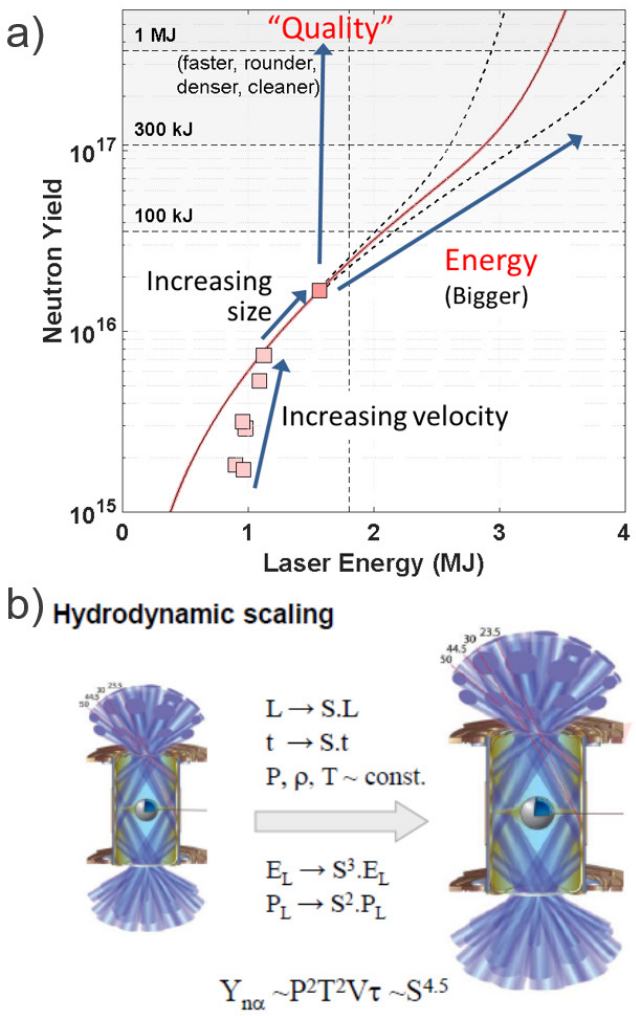

Figure 9. (*a*) Estimated neutron yield based on no burn scaling from HDC data in pink with estimates for alpha self-heating. Black dashed curves represent notional bounds [37, 50]. (*b*) Hydrodynamic target scaling.

mixing at the ablator/ice interface has a strong dependence on the dopant buried a few microns insider the inner surface of the capsule, which moderates the Atwood number by reducing pre-heating by Au m-band emission from the hohlraum. This is illustrated in figure 8 by simulations which show a more stable interface in the target that contains the dopant and a corresponding increase in performance [87, 88]. High resolution velocimetry measurements of the expansion of the rear surface of ablator materials has shown that perturbations may be seeded by the microstructure in crystalline materials such as beryllium and diamond [89] and is sensitive to both the crystalline structure and shock pressure. Efforts are underway to develop techniques that can measure mix at high convergence ratios (~10–20) related to the ablator/ice interfaces using x-ray self-emission backlighting [90, 91], high resolution imaging with a spherical crystal imager [92], and cylindrical implosion platforms [93].

4. Scaling

Another means to improve target performance is increasing the size of the target, i.e. scaling both hohlraum and capsule, while preserving all other properties. A linear scaling of the target hydrodynamically scales the capsule size, i.e. scaling with sound speed transit times, preserving the implosion dynamics [94]. This does assume the capsule drive provided by the hohlraum also scales which has not been demonstrated. Using this scaling, the yield without alpha heating, i.e. no burn, scale as $Y \sim S^{4.5}$, where Y is neutron yield and S is scale, due to the increase in the volume of the burn region, the additional confinement time due to the sound speed crossing time of the disassembly of the implosion and less thermal conduction losses. Combining the no alpha heating scaling with a model for alpha capture and using the hydro-scaling for the laser energy, $E \sim S^3$, and power, $P \sim S^2$, a curve based on the performance of an experiment can be derived as shown in figure 9(*a*). The laser energy axis provides an estimate of the laser energy needed for the current quality implosions to reach a given yield. At laser energies near 3 MJ, implosions can enter a burning plasma phase in which the alpha heating exceed all loss mechanisms. At laser energies in the range of 3.5–4 MJ, gains greater than one may be achieved. These estimates are based on the current quality of HDC implosions on NIF represented by the data points in pink. The caveat to these estimates is that some processes and target parameters do not hydro-scale, chief amongst these being alpha-heating and laser matter interactions including laser plasma instabilities. These are highly non-linear processes which add significant uncertainty to the simple analytic estimate. The impact of these processes, as well as other mechanisms that do not scale hydrodyanmically, are being investigated to determine how they affect target performance with increased size. In additions, it should be noted that work is ongoing to develop ways to increase the capsule size without increasing the hohlraum size which could lead to greater target performance for any given laser energy and power. The real challenge to the scaling is estimating the level of confidence which becomes more uncertain as the estimates move away from the region where data is available. This is shown by the black dashed lines in figure 9 which are notional at this time.

A significant effort to interpret and utilize the data to quantify the uncertainties for the scaling is underway. Uncertainty quantification beyond regions where data is available is a field of study unto itself. The work along with utilizing state of the art tools such as machine learning is being applied to this problem for ICF. Large ensembles of simulations with machine learning techniques are being used to determine the principle metrics for ICF implosion performance [95–99]. Large ensembles of simulation output and experimental data are being coupled with machine learning techniques to propagate and incorporate uncertainty in predictions to new regimes, assessing and evaluating competing

hypotheses for performance in the face of statistical, experimental and numerical uncertainties.

Concurrently, with the experimental efforts to improve ICF performance, work is ongoing to improve laser performance generating higher laser energy and power. As technology progresses and understanding of laser damage/mitigation advances [100], possible paths to increasing the laser energy at 351 nm are being investigated, and there is an option to move the 527 nm laser light which should exceed 4 MJ [101–103]. Increased laser energy enables larger hohlraums and capsules to be driven as a means to improve performance with the caveat that laser plasma instabilities specifically stimulated Brillouin scattering at late times is still an unknown risk.

5. Conclusions

Considerable progress has been made toward thermonuclear ICF ignition over the past eight years, but many challenges remain. The highly integrated multi-physics nature of ICF makes it difficult to identify all physics mechanisms that may be degrading performance or inadequacies in models due to compensating and coupling between effects. The strategy going forward is to continue to identify and to address phenomena that affect implosion quality, namely 3D effects due to both low and high mode asymmetries. Efforts will continue to address identified remaining low mode asymmetries while making an asserted effort to address high mode mix. This entails reducing the effect of engineering features and addressing other sources of mix. Due to the difficulty in measuring mix for high convergence system and ongoing research into the understanding of mix, this effort will be a focus for the near future since time is needed to determine what is missing in our understanding. There is a concurrent effort to increase the capsule size in an attempt to couple more energy to the fuel to increase performance. Once the 1D nature of the implosion is improved it may also be possible to further stress implosion velocity and convergence ratio to increase performance without 3D effects negating any gains. This will require improved drivers to maintain symmetry control with bigger capsules. All of these efforts will feed into design that can utilize higher laser energies when available to scale up the targets.

Acknowledgment

This work performed under the auspices of the U.S. Department of Energy by Los Alamos National Laboratory under contract DE-AC52-06NA25396, by Lawrence Livermore National Laboratory under Contract DE-AC52-07NA27344, General Atomics, and the Massachusetts Institute of Technology.

ORCID iDs

L.F. Berzak Hopkins https://orcid.org/0000-0002-9187-5667
O.A. Hurricane https://orcid.org/0000-0002-8600-5448
O.S. Jones https://orcid.org/0000-0002-0372-7657

References

[1] Lindl J. 1995 Development of the indirect-drive approach to inertial confinement fusion and the target physics basis for ignition and gain *Phys. Plasmas* **2** 3933
[2] Wilson D.C. *et al* 1998 The development and advantages of beryllium capsules for the National Ignition Facility *Phys. Plasmas* **5** 1953
[3] Haan S.W. *et al* 2004 Design and simulations of indirect drive ignition targets for NIF *Nucl. Fusion* **44** S171
[4] Haan S.W. *et al* 2013 NIF ignition campaign target perpormance and requirements: status May 2012 *Fusion Sci. Technol.* **63** 67
[5] Haan S.W. *et al* 2016 Update 2015 on target fabrication requirements for NIF layered implosions, with emphasis on capsule support and oxygen modulations in GDP *Fusion Sci. Technol.* **70** 121
[6] Stephens R.B., Haan S.W. and Wilson D.C. 2002 Characterization specifications for baseline indirect drive NIF targets *Fusion Sci. Technol.* **41** 226
[7] Paisner J.A., Campbell E.M. and Hogan W.J. 1994 The National Ignition Facility project *Fusion Technol.* **26** 755
[8] Glenzer S.H. *et al* 2012 Cryogenic thermonuclear fuel implosions on the National Ignition Facility *Phys. Plasmas* **19** 056318
[9] Glenzer S.H. *et al* 2012 First implosion experiments with cryogenic thermonuclear fuel on the National Ignition Facility *Plasma Phys. Control. Fusion* **54** 045013
[10] Haan S.W. *et al* 2011 Point design targets, specifications, and requirements for the 2010 ignition campaign on the National Ignition Facility *Phys. Plasmas* **18** 051001
[11] Ma T. *et al* 2013 Onset of hydrodynamic mix in high-velocity, highly compressed inertial confinement fusion implosions *Phys. Rev. Lett.* **111** 085004
[12] Regan S.P., *et al* 2013 Hot-spot mix in ignition-scale inertial confinement fusion targets *Phys. Rev. Lett.* **111** 045001
[13] Haan S.W. 1991 Weakly nonlinear hydrodynamic instabilities in inertial fusion *Phys. Fluids* B **3** 2349
[14] Hoffman N.M. 1995 Hydrodynamic instabilities in inertial confinement fusion *Laser Plasma Interactions 5: Inertial Confinement Fusion* ed M.B. Hooper vol 45 (Edinburgh: Scottish Univ Summer School Physics Publications) pp 105–37
[15] Kilkenny J.D. *et al* 1993 Experimental-determination of the hydrodynamic instability growth-rates in indirect and direct-drive ICF *Plasma Physics and Controlled Nuclear Fusion Research 1992* vol 3 pp 133–42
[16] Town R.P.J. *et al* 2014 Dynamic symmetry of indirectly driven inertial confinement fusion capsules on the National Ignition Facility *Phys. Plasmas* **21** 056313
[17] Edwards M.J. *et al* 2013 Progress towards ignition on the National Ignition Facility *Phys. Plasmas* **20** 070501
[18] Clark D.S. *et al* 2013 Detailed implosion modeling of deuterium-tritium layered experiments on the National Ignition Facility *Phys. Plasmas* **20** 056318
[19] Hurricane O.A. *et al* 2014 The high-foot implosion campaign on the National Ignition Facility *Phys. Plasmas* **21** 056314
[20] Dittrich T.R. *et al* 2014 Design of a high-foot high-adiabat ICF capsule for the National Ignition Facility *Phys. Rev. Lett.* **112** 055002
[21] Hurricane O.A. *et al* 2014 Fuel gain exceeding unity in an inertially confined fusion implosion *Nature* **506** 343
[22] Park H.S. *et al* 2014 High-adiabat high-foot inertial confinement fusion implosion experiments on the National Ignition Facility *Phys. Rev. Lett.* **112** 055001

[23] Peterson J.L., Michel P., Thomas C.A. and Town R.P.J. 2014 The impact of laser plasma interactions on three-dimensional drive symmetry in inertial confinement fusion implosions *Phys. Plasmas* **21** 072712

[24] Kruer W.L., Wilks S.C., Afeyan B.B. and Kirkwood R.K. 1996 Energy transfer between crossing laser beams *Phys. Plasmas* **3** 382

[25] Michel P. *et al* 2009 Tuning the implosion symmetry of ICF targets via controlled crossed-beam energy transfer *Phys. Rev. Lett.* **102** 025004

[26] Michel P. *et al* 2010 Symmetry tuning via controlled crossed-beam energy transfer on the National Ignition Facility *Phys. Plasmas* **17** 056305

[27] Moody J.D. *et al* 2014 Progress in hohlraum physics for the National Ignition Facility *Phys. Plasmas* **21** 056317

[28] Clark D.S. *et al* 2016 Three-dimensional simulations of low foot and high foot implosion experiments on the National Ignition Facility *Phys. Plasmas* **23** 056302

[29] Nagel S.R. *et al* 2015 Effect of the mounting membrane on shape in inertial confinement fusion implosions *Phys. Plasmas* **22** 022704

[30] Tommasini R. *et al* 2015 Tent-induced perturbations on areal density of implosions at the National Ignition Facility *Phys. Plasmas* **22** 056315

[31] Meezan N.B. *et al* 2017 Indirect drive ignition at the National Ignition Facility *Plasma Phys. Control. Fusion* **59** 014021

[32] Callahan D. 2018 Low gas-fill density ignition hohlraums on the National Ignition Facility *Stockpile Stewardship Q.* **6** 4

[33] Hopkins L.F.B. *et al* 2015 Near-vacuum hohlraums for driving fusion implosions with high density carbon ablators *Phys. Plasmas* **22** 056318

[34] Hopkins L.F.B. *et al* 2015 First high-convergence cryogenic implosion in a near-vacuum hohlraum *Phys. Rev. Lett.* **114** 175001

[35] Meezan N.B. *et al* 2015 Cryogenic tritium–hydrogen–deuterium and deuterium–tritium layer implosions with high density carbon ablators in near-vacuum hohlraums *Phys. Plasmas* **22** 062703

[36] Le Pape S. *et al* 2016 The near vacuum hohlraum campaign at the NIF: a new approach *Phys. Plasmas* **23** 056311

[37] Le Pape S. *et al* 2018 Fusion energy output greater than the kinetic energy of an imploding shell at the National Ignition Facility *Phys. Rev. Lett.* **120** 245003

[38] Betti R. *et al* 2010 Thermonuclear ignition in inertial confinement fusion and comparison with magnetic confinement *Phys. Plasmas* **17** 058102

[39] Cheng B.L., Kwan T.J.T., Wang Y.M. and Batha S.H. 2014 On thermonuclear ignition criterion at the National Ignition Facility *Phys. Plasmas* **21** 102707

[40] Lawson J.D. 1957 Some criteria for a power producing thermonuclear reactor *Proc. Phys. Soc.* B **70** 6

[41] Chang P. *et al* 2010 Generalized measurable ignition criterion for inertial confinement fusion *Phys. Rev. Lett.* **104** 135002

[42] Zhou C.D. and Betti R. 2008 A measurable Lawson criterion and hydro-equivalent curves for inertial confinement fusion *Phys. Plasmas* **15** 102707

[43] Loomis E.N. *et al* 2018 Implosion shape control of high-velocity, large case-to-capsule ratio beryllium ablators at the National Ignition Facility *Phys. Plasmas* **25** 072708

[44] Zylstra A.B. *et al* 2018 Beryllium capsule implosions at a case-to-capsule ratio of 3.7 on the National Ignition Facility *Phys. Plasmas* **25** 102704

[45] Zylstra A.B. *et al* 2019 Implosion performance of subscale beryllium capsules on the NIF *Phys Plasmas* **26** 052707

[46] Jones O.S. *et al* 2017 Progress towards a more predictive model for hohlraum radiation drive and symmetry *Phys. Plasmas* **24** 056312

[47] Ralph J.E. *et al* 2018 The influence of hohlraum dynamics on implosion symmetry in indirect drive inertial confinement fusion experiments *Phys. Plasmas* **25** 082701

[48] Izumi N. *et al* 2018 Simultaneous visualization of wall motion, beam propagation, and implosion symmetry on the National Ignition Facility *Rev. Sci. Instrum.* **89** 10K111

[49] Callahan D.A. *et al* 2018 Exploring the limits of case-to-capsule ratio, pulse length, and picket energy for symmetric hohlraum drive on the National Ignition Facility laser *Phys. Plasmas* **25** 056305

[50] Divol L. *et al* 2017 Symmetry control of an indirectly driven high-density-carbon implosion at high convergence and high velocity *Phys. Plasmas* **24** 056309

[51] Hall G.N. *et al* 2017 The relationship between gas fill density and hohlraum drive performance at the National Ignition Facility *Phys. Plasmas* **24** 052706

[52] Turnbull D. *et al* 2016 *Phys. Plasmas* **23** 052710

[53] Kritcher A.L. *et al* 2014 Metrics for long wavelength asymmetries in inertial confinement fusion implosions on the National Ignition Facility *Phys. Plasmas* **21** 042708

[54] Spears B.K. *et al* 2014 Mode 1 drive asymmetry in inertial confinement fusion implosions on the National Ignition Facility *Phys. Plasmas* **21** 042702

[55] Bleuel D.L. *et al* 2012 Neutron activation diagnostics at the National Ignition Facility *Rev. Sci. Instrum.* **83** 10D313

[56] Yeamans C.B. and Bleuel D.L. 2017 The spatially distributed neutron activation diagnostic FNADs at the National Ignition Facility *Fusion Sci. Technol.* **72** 120

[57] Yu V. *et al* 2010 The National Ignition Facility neutron time-of-flight system and its initial performance *Rev. Sci. Instrum.* **81** 10D325

[58] Lerche R.A. *et al* 2010 National Ignition Facility neutron time-of-flight measurements *Rev. Sci. Instrum.* 10D319

[59] Johnson M.G. *et al* 2016 Indications of flow near maximum compression in layered deuterium-tritium implosions at the National Ignition Facility *Phys. Rev.* E **94** 021202

[60] Rinderknecht H.G., Bionta R., Grim G., Hatarik R., Khater H., Schlossberg D. and Yeamans C. 2018 Velocity correction for neutron activation diagnostics at the NIF *Rev. Sci. Instrum.* **89** 10i125

[61] Merrill F.E. *et al* 2012 The neutron imaging diagnostic at NIF (invited) *Rev. Sci. Instrum.* **83** 10D317

[62] Volegov P.L., Danly C.R., Fittinghoff D., Geppert-Kleinrath V., Grim G., Merrill F.E. and Wilde C.H. 2017 Three-dimensional reconstruction of neutron, gamma-ray, and x-ray sources using spherical harmonic decomposition *J. Appl. Phys.* **122** 175901

[63] Tommasini R. *et al* 2011 Development of Compton radiography of inertial confinement fusion implosions *Phys. Plasmas* **18** 056309

[64] Tommasini R. *et al* 2017 Short pulse, high resolution, backlighters for point projection high-energy radiography at the National Ignition Facility *Phys. Plasmas* **24** 053104

[65] Nora R., Field J.E., Young C., Mariscal D., Ma T.Y.W. and Spears B.K. 2018 3D HYDRA capsule studies on the effect of hohlraum windows *Bull. Am. Phys. Soc.* (http://meetings.aps.org/link/BAPS.2018.DPP.BO6.4)

[66] Ma T. *et al* 2018 Experimental investigation of the source of mode one asymmetries in indirect-drive ICF implosions* *Bull. Am. Phys. Soc.* (http://meetings.aps.org/link/BAPS.2018.DPP.BO6.11)

[67] Landen O. 2018 personal communication

[68] Bhandarkar S. *et al* 2018 Fabrication of low-density foam liners in hohlraums for NIF targets *Fusion Sci. Technol.* **73** 194

[69] Xu Y., Zhu T., Li S. and Yang J. 2011 Beneficial effect of CH foam coating on x-ray emission from laser-irradiated high-*Z* material *Phys. Plasmas* **18** 053301

[70] Amendt P., Cerjan C., Hinkel D.E., Milovich J.L., Park H.S. and Robey H.F. 2008 Rugby-like hohlraum experimental designs for demonstrating x-ray drive enhancement *Phys. Plasmas* **15** 012702

[71] Vandenboomgaerde M., Bastian J., Casner A., Galmiche D., Jadaud J.P., Laffite S., Liberatore S., Malinie G. and Philippe F. 2007 Prolate-spheroid ('rugby-shaped') hohlraum for inertial confinement fusion *Phys. Rev. Lett.* **99** 065004

[72] Amendt P. *et al* 2014 Low-adiabat rugby hohlraum experiments on the National Ignition Facility: comparison with high-flux modeling and the potential for gas-wall interpenetration *Phys. Plasmas* **21** 112703

[73] Masson-Laborde P.E. *et al* 2016 Laser plasma interaction on rugby hohlraum on the Omega Laser Facility: comparisons between cylinder, rugby, and elliptical hohlraums *Phys. Plasmas* **23** 022703

[74] Robey H.F., Hopkins L.B., Milovich J.L. and Meezan N.B. 2018 The I-Raum: a new shaped hohlraum for improved inner beam propagation in indirectly-driven ICF implosions on the National Ignition Facility *Phys. Plasmas* **25** 012711

[75] Martinez D.A. *et al* 2017 Hydro-instability growth of perturbation seeds from alternate capsule-support strategies in indirect-drive implosions on National Ignition Facility *Phys. Plasmas* **24** 102707

[76] Weber C.R. *et al* 2017 Improving ICF implosion performance with alternative capsule supports *Phys. Plasmas* **24** 056302

[77] Smalyuk V.A. *et al* 2014 First measurements of hydrodynamic instability growth in indirectly driven implosions at ignition-relevant conditions on the National Ignition Facility *Phys. Rev. Lett.* **112** 185003

[78] MacPhee A.G. *et al* 2018 Hydrodynamic instabilities seeded by the x-ray shadow of ICF capsule fill-tubes *Phys. Plasmas* **25** 082702

[79] MacPhee A.G. *et al* 2018 Mitigation of x-ray shadow seeding of hydrodynamic instabilities on inertial confinement fusion capsules using a reduced diameter fuel fill-tube *Phys. Plasmas* **25** 054505

[80] Pak A. *et al* 2017 Assessment of the impact that the capsule fill tube has on implosions conducted with high density carbon ablators *Bull. Am. Phys. Soc.* PO7.00005 (http://meetings.aps.org/link/BAPS.2017.DPP.PO7.5)

[81] Smalyuk V.A. *et al* 2018 Review of hydro-instability experiments with alternate capsule supports in indirect-drive implosions on the National Ignition Facility *Phys. Plasmas* **25** 072705

[82] Hammel B.A. *et al* 2018 A 'polar contact' tent for reduced perturbation and improved performance of NIF ignition capsules *Phys. Plasmas* **25** 082714

[83] Biener J. *et al* 2009 Diamond spheres for inertial confinement fusion *Nucl. Fusion* **49** 112001

[84] MacKinnon A.J. *et al* 2014 High-density carbon ablator experiments on the National Ignition Facility *Phys. Plasmas* **21** 056318

[85] Takabe H., Mima K., Montierth L. and Morse R.L. 1985 Self-consistent growth rate of the Rayleigh-Taylor instability in an ablatively accelerating plasma *Phys. Fluids* **28** 3676

[86] Haines B.M. *et al* 2017 The effects of convergence ratio on the implosion behavior of DT layered inertial confinement fusion capsules *Phys. Plasmas* **24** 072709

[87] Hopkins L.B. *et al* 2018 Increasing stagnation pressure and thermonuclear performance of inertial confinement fusion capsules by the introduction of a high-*Z* dopant *Phys. Plasmas* **25** 080706

[88] Hopkins L.B. *et al* 2019 Toward a burning plasma state using diamond ablator inertially confined fusion (ICF) implosions on the National Ignition Facility (NIF) *Plasma Phys. Control. Fusion* **61** 014023

[89] Ali S.J. *et al* 2018 Probing the seeding of hydrodynamic instabilities from nonuniformities in ablator materials using 2D velocimetry *Phys. Plasmas* **25** 092708

[90] Pickworth L.A. *et al* 2016 Measurement of inflight shell areal density near peak velocity using a self backlighting technique *J. Phys.: Conf. Ser.* **717** 012044

[91] Pickworth L.A. *et al* 2018 Visualizing deceleration-phase instabilities in inertial confinement fusion implosions using an 'enhanced self-emission' technique at the National Ignition Facility *Phys. Plasmas* **25** 054502

[92] Hall G.N. *et al* 2019 The Crystal Backlighter Imager: a spherically bent crystal imager for radiography on the National Ignition Facility *Rev. Sci. Instrum.* **90** 013702

[93] Palaniyappan S. *et al* 2018 *Phys. Plasmas* in preparation

[94] Nora R. *et al* 2014 Theory of hydro-equivalent ignition for inertial fusion and its applications to OMEGA and the National Ignition Facility *Phys. Plasmas* **21** 056316

[95] Bremer P.-T., Maljovec D., Saha A., Wang B., Gaffney J., Spears B.K. and Pascucci V. 2015 ND^{2}AV: N-dimensional data analysis and visualization analysis for the National Ignition Campaign *Comput. Vis. Sci.* **17** 1

[96] Langer S.H., Spears B., Peterson J.L., Field J.E., Nora R., Brandon S. and IEEE 2016 A Hydra UQ workflow for NIF ignition experiments *Proc. of ISAV 2016: 2nd Workshop on in situ Infrastructures for Enabling Extreme-Scale Analysis and Visualization (Salt Lake City, UT, 13–18 November 2016)* (IEEE Press: Piscataway, NJ) pp 1–6 (http://sc16.supercomputing.org)

[97] Nora R., Peterson J.L., Spears B.K., Field J.E. and Brandon S. 2017 Ensemble simulations of inertial confinement fusion implosions *Stat. Anal. Data Mining* **10** 230

[98] Humbird K.D., Peterson J.L. and McClarren R.G. 2018 Deep neural network initialization with decision trees *IEEE Trans. Neural Netw. Learn. Syst.* **30** 1286

[99] Peterson J.L., Humbird K.D., Field J.E., Brandon S.T., Langer S.H., Nora R.C., Spears B.K. and Springer P.T. 2017 Zonal flow generation in inertial confinement fusion implosions *Phys. Plasmas* **24** 032702

[100] Stolz C.J. *et al* 2018 Transport mirror laser damage mitigation technologies on the National Ignition Facility *Proc. SPIE* **10691** 106910W

[101] Suter L.J. *et al* 2004 Prospects for high-gain, high yield National Ignition Facility targets driven by 2 omega (green) light *Phys. Plasmas* **11** 2738

[102] Manes K.R. *et al* 2016 Damage mechanisms avoided or managed for NIF large optics *Fusion Sci. Technol.* **69** 146

[103] Spaeth M.L. *et al* 2016 Optics recycle loop strategy for NIF operations above UV laser-induced damage threshold *Fusion Sci. Technol.* **69** 25